Geomorphic controls on hyporheic exchange flow in mountain streams

Tamao Kasahara[1]

Department of Forest Science, Oregon State University, Corvallis, Oregon, USA

Steven M. Wondzell

Pacific Northwest Research Station, Olympia Forestry Sciences Laboratory, Olympia, Washington, USA

[1] Hyporheic exchange flows were simulated using MODFLOW and MODPATH to estimate relative effects of channel morphologic features on the extent of the hyporheic zone, on hyporheic exchange flow, and on the residence time of stream water in the hyporheic zone. Four stream reaches were compared in order to examine the influence of stream size and channel constraint. Within stream reaches, the influence of pool-step or pool-riffle sequences, channel sinuosity, secondary channels, and channel splits was examined. Results showed that the way in which channel morphology controlled exchange flows differed with stream size and, in some cases, with channel constraint. Pool-step sequences drove hyporheic exchange in the second-order sites, creating exchange flows with relatively short residence times. Multiple features interacted to drive hyporheic exchange flow in the unconstrained fifth-order site, where pool-riffle sequences and a channel split created exchange flows with short residence times, whereas a secondary channel created exchange flows with long residence times. There was relatively little exchange flow in the bedrock-constrained fifth-order site. Groundwater flow models were effective in examining the morphologic features that controlled hyporheic exchange flow, and surface-visible channel morphologic features controlled the development of the hyporheic zone in these mountain streams.   *INDEX TERMS:* 1824 Hydrology: Geomorphology (1625); 1829 Hydrology: Groundwater hydrology; 1860 Hydrology: Runoff and streamflow; *KEYWORDS:* hyporheic zone, stream geomorphology, groundwater flow models

1. Introduction

[2] Stream water may flow into shallow, near-stream sediment and return to the stream channel over relatively short distances. This movement of stream water is called hyporheic exchange flow and defines the hyporheic zone (e.g., the saturated subsurface area containing stream water). Recent research has shown that the hyporheic zone plays an important role in many stream ecosystems. Exchange flows of oxygenated stream water transport nutrients and dissolved organic carbon into the hyporheic zone [*Grimm and Fisher*, 1984; *Wondzell and Swanson*, 1996b; *Kaplan and Newbold*, 2000; *Mulholland et al.*, 2000], where relatively long residence times and contact with microbes in sediment leads to extensive biological activity and transformation of nutrients [*Triska et al.*, 1993b; *Jones et al.*, 1995; *Findlay*, 1995; *Holmes et al.*, 1996]. These nutrient transformations are especially important in stream nitrogen cycles, where return flows of hyporheic water transport inorganic forms back to the stream. Several studies have shown that the hyporheic zone is an important source of inorganic nitrogen in nitrogen-limited streams [*Triska et al.*, 1993a; *Holmes et al.*, 1994; *Jones et al.*, 1995; *Wondzell and Swanson*, 1996b]. However, quantifying the relative effect of hyporheic processes on stream ecosystems remains difficult because the measurement of the amount of hyporheic exchange flow and the residence time distribution of water in the hyporheic zone is not easy.

[3] The influence of channel morphologic features on the formation of hyporheic zones has received considerable attention. Changes in longitudinal gradients in step-pool and riffle-pool sequences drive small-scale exchange flows vertically through the streambed, as well as laterally through stream banks [*Harvey and Bencala*, 1993; *Hill et al.*, 1998]. Exchanges at larger spatial scales are influenced by channel sinuosity and the flow of stream water through point bars [*Vervier et al.*, 1993; *Wroblicky et al.*, 1998]; secondary channels [*Wondzell and Swanson*, 1996a; *Wondzell and Swanson*, 1999]; preferential flow through buried, or "paleochannels" [*Stanford and Ward*, 1988]; and finally, change in channel constraint at the upper and lower ends of bounded alluvial reaches [*Stanford and Ward*, 1993; *Fernald et al.*, 2001]. These studies show that a wide variety of channel morphologic features create head gradients that drive the advection of stream water along flow paths

[1]Now at Department of Geography, York University, Toronto, Ontario, Canada.

through shallow streamside aquifers. However, none of these studies examined the relative effects of multiple features on hyporheic exchange flow.

[4] Numerical groundwater flow models, like MOD-FLOW [*McDonald and Harbaugh*, 1988], have long been used to simulate groundwater flow at large spatial scales [*Wang and Anderson*, 1982; *Anderson and Woessner*, 1992] and have also been applied to smaller spatial scales [*Stoertz and Bradbury*, 1989]. Recently, *Wondzell and Swanson* [1996a] and *Wroblicky et al.* [1998] have used the two-dimensional version of MODFLOW to simulate hyporheic exchange flows through near-stream aquifers. Model simulations accurately predicted the location of gaining and losing stream reaches [*Wroblicky et al.*, 1998] and the spatial extent of the hyporheic zone and the direction of flow paths [*Wondzell and Swanson*, 1996a]. Additionally, residence time of hyporheic water was measured by coupling the results of MODFLOW analysis with a particle-tracking module [*Wroblicky et al.*, 1998].

[5] The combination of studies of visible stream geomorphic features and the use of numerical groundwater flow models may offer a possible way to explore factors controlling hyporheic exchange flows in stream networks. If groundwater flow models, like the modular three-dimensional finite difference groundwater flow model (MOD-FLOW), can accurately relate hyporheic exchange flow to channel morphology, examination of visible geomorphic features may allow expansion of hyporheic research from the reach scale to the stream network scale.

[6] The objective of this study was to investigate the relative influence of channel and valley-floor morphologic features on the development of hyporheic zones in mountain streams. Groundwater flow models were used in combination with field measurements to examine (1) the horizontal extent of the hyporheic zone; (2) the hyporheic exchange flow (Q_{HEF}; expressed in units of discharge, i.e., l/s); and (3) the residence time distribution of stream water in the hyporheic zone (HEF_{RT}). Streams of different size (second- and fifth-order) and with varying valley constraint (constrained versus unconstrained) were compared. Within each stream type, we examined the relative importance of changes in channel gradient, channel sinuosity, and the influence of secondary channels and split channels around islands on the hyporheic zone. We used sensitivity analysis to identify the relative effect of morphologic features on the development of the hyporheic zone in each stream type. Finally, the sensitivity analysis was extended to include a representative range in the size and frequency of geomorphic features, measured from extensive surveys of other second- and fifth-order mountain-stream reaches.

2. Study Sites

[7] This study was conducted in the main stem of Lookout Creek and in two of its tributary streams, WS01 and WS03, which are located in the H. J. Andrews Experimental Forest (44°20′N, 122°20′W) in the western Cascade mountains of Oregon, United States. Elevations within the Lookout Creek watershed range from 428 to 1620 m. Average annual precipitation ranges between 2300 and 3550 mm, depending on the elevation, and falls mainly from November to March [*Bierlmaier and McKee*, 1989]. The watersheds are forested, primarily with Douglas fir

Table 1. Geomorphic Characteristics of Each Well Network Site

	WS01	WS03	Middle Lookout	Bedrock-Constrained
Site length, m	72	65	215	114
Wetted channel width, m	2.3	2.3	9.4	9.2
Valley/active channel width, m	14.9	6.9	44.8	17.6
Channel gradient, m/m	0.14	0.13	0.02	0.01
Sinuosity, m/m	1.3	1.3	1.3	1.1
Number of steps/riffles	9	10	6	1
Contribution of steps/riffles to change in elevation, %	63.3	75.5	65.5	41.7
Saturated hydraulic conductivity, cm/s	0.007	0.007	0.153	0.065

(*Psudotsuga menziesii*), western hemlock (*Tsuga heterophylla*), and western red cedar (*Thuja plicata*). Red alder (*Alnus rubra* Bong.) and willow (*Salix* spp.) are common riparian, deciduous trees.

[8] Two study reaches, the Middle Lookout site and the Bedrock-constrained site, were located along the main stem of Lookout Creek, a fifth-order stream draining a catchment of 6400 ha. Study reaches were also located in WS01 and WS03, second-order tributaries of Lookout Creek that drain areas of 95.9 and 101.1 ha, respectively. The valley floors of Middle Lookout and WS01 are wide, relative to the width of the wetted channel. We define these sites as unconstrained because they are at least twice as wide as the valley floors of their comparison sites, the Bedrock-constrained site and WS03, which we define as constrained (Table 1).

3. Methods
3.1. Field Measurements

[9] Well networks at the Middle Lookout and the Bedrock-constrained sites on lower Lookout Creek were established during the summer of 1996, and the well networks in WS01 and WS03 were installed during the summer of 1997. Wells were located so as to provide good spatial resolution of subsurface flows. The spacing between wells varied in proportion to the width of the wetted channel and length of channel units at each study site (Figures 1 and 2).

[10] Well casings were made from PVC pipe that was "screened" by drilling 0.32-cm-diameter holes into the bottom of each pipe. Wells located in the wetted stream channel were screened over a 5-cm interval. All other wells were screened over a 50-cm interval. Wells were driven by hand because the study sites lacked road access. Large boulders hindered well placement so that most wells penetrated to 1 m or less below the ground surface, and the deepest wells penetrated only a little over 2 m.

[11] The locations of all wells, primary, secondary, and back channels, and the edges of the active valley floor were surveyed and mapped to scale (Figures 1 and 2). The elevation of well heads and the ground level at each well were surveyed. Longitudinal profiles of stream channels, showing both the stream bed and stream water elevations, were also surveyed at 1-m intervals, except in runs or glides of fifth-order streams, where points were spaced at 2- to 5-m intervals. Water table elevations were recorded from the well networks soon after surveys were completed. Saturated hydraulic conductivities were estimated at each well using a falling-head slug test and the *Bouwer and Rice* [1976] analysis method.
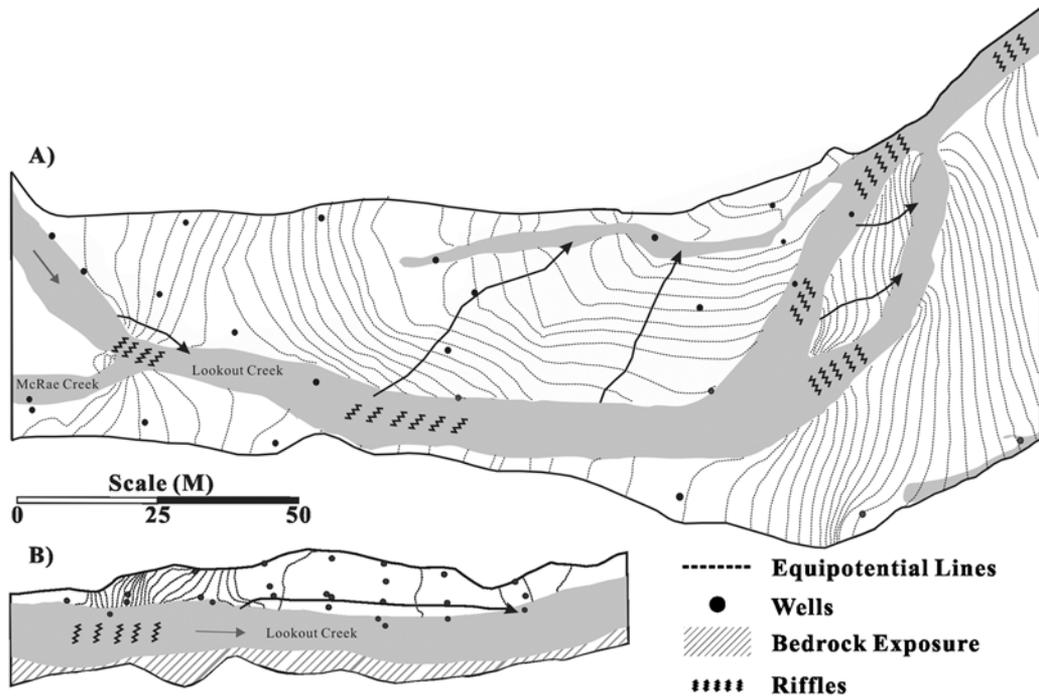
Figure 1. Site maps of (a) the Middle Lookout Creek study site and (b) the Bedrock-constrained site. Water table elevations are predicted from MODFLOW simulations and shown as equipotential lines (0.1 m interval).

[12] Extensive stream surveys were conducted to obtain a more representative characterization of channel and valley-floor morphologic features present in the streams studied. We surveyed a total of 1450 m of unconstrained and 300 m of constrained fifth-order stream channels and 200 m of unconstrained and 220 m of constrained second-order stream channels. Stream water elevations were measured every 1–2 m in second-order streams and every 5–10 m in
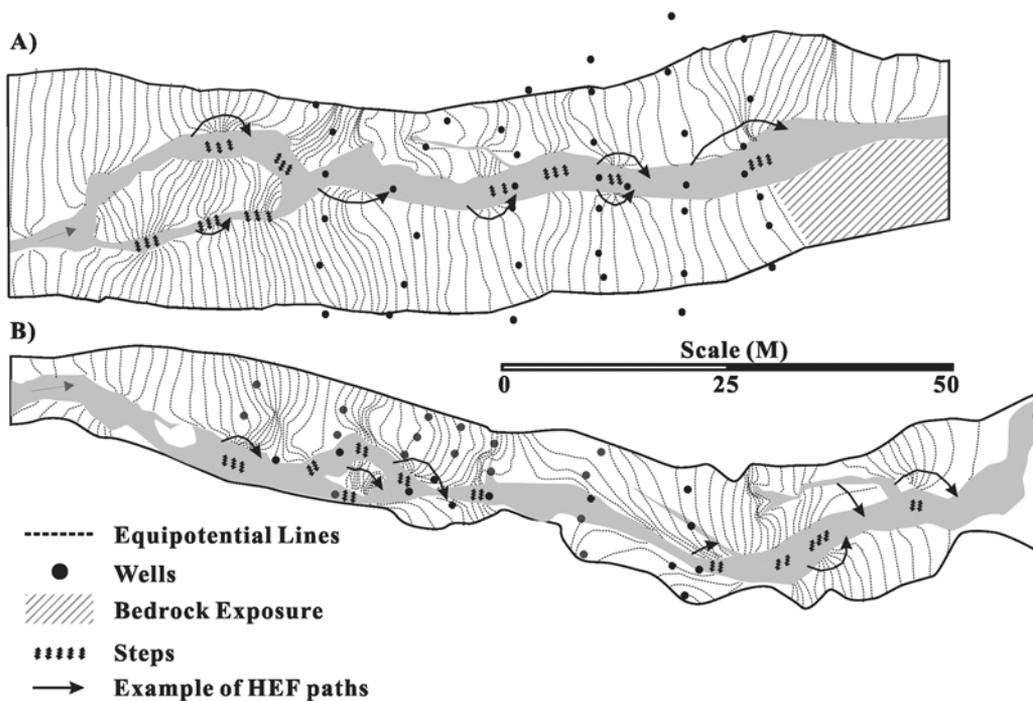

Figure 2. Site maps of (a) the WS01 study site and (b) the WS03 site. Water table elevations are predicted from MODFLOW simulations and shown with equipotential lines (0.1 m interval).

fifth-order streams. Longitudinal profiles of all secondary and back channels within the study reaches were also surveyed. The surveyed stream reaches were divided into representative survey lengths (RSLs) with lengths approximately 20 times the width of the wetted channel. The resulting RSLs were 160 m in the Lookout Creek sites and 30 m in WS01 and WS03. Channel and valley-floor morphologic features were tallied in each RSL. Steps and riffles were defined as locations where longitudinal gradient exceeded 1.5 times the average channel gradient of the study reach. Contribution of steps to streambed gradient was calculated by dividing change in elevation created by steps by the total change in elevation within the RSL. Channel sinuosity was calculated by dividing wetted-channel length by the RSL. The length of secondary channels and channel splits was recorded, and cross-valley gradients between these channels were calculated.

3.2. Model Simulations of Well Network Sites

[13] Three dimensional groundwater flow models were built for each well network site to simulate water exchange between the stream and the underlying unconfined aquifer using MODFLOW [McDonald and Harbaugh, 1988]. Data from each well network site were used to parameterize groundwater flow models. Models were calibrated to fit water table elevations observed from the wells. Model simulations were conducted only for base flow conditions when we assumed that the shape of the water table would be in equilibrium with lateral groundwater inputs. This assumption is supported by observation of the water table from the well network sites, the shape and elevation of which changed little over base flow periods. Therefore all simulations were conducted under steady state conditions.

[14] Model domains consisted of five-layer block-center finite difference grids. The cells were square, measuring 0.5 m and 0.3 m in fifth-order and second-order streams, respectively. Average wetted-channel depths were 0.3 m in fifth-order stream and 0.15 m in second-order stream so that depths of cells in the first layer were 0.3 and 0.15 m, respectively. Stream channels were modeled using constant-head cells, such that cells of the uppermost model layer, located within the wetted stream channel, were assigned constant head values equal to the stream water elevation measured in the longitudinal survey. Morphologic features were represented by the location of these constant-head (or stream) cells and the assigned head values. For example, riffles were represented by steep head gradients in a series of constant-head cells. Constant-head cells were also used in upstream and downstream boundaries of the model domain, whereas side boundaries were modeled using the combination of variable-flow and no-flow boundaries.

[15] Bedrock outcrops at valley margins, and bedrock exposed in the streambed, suggest that aquifers are relatively shallow, but also suggest that the bedrock surface is uneven. The thickness of the aquifers at the well network sites was not surveyed, however. We arbitrarily set the saturated thickness of the aquifer as 4.2 m in fifth-order streams and 2.15 m in second-order streams. Slug tests showed that the aquifer was heterogeneous, and therefore saturated hydraulic conductivity measured in slug tests was interpolated to the region surrounding each well using the Thessin Polygon method. Leakage was calculated from the

saturated hydraulic conductivity and the size of the grid cells [Engineering Computer Graphic Laboratory, 1998] and also interpolated to the model domain using the Thessin Polygon method. Finally, we assumed the aquifer was isotropic.

[16] Calibrated models were used to generate contour maps of water table equipotentials from which we estimated length and direction of subsurface flow paths and the areal extent of the hyporheic zone. The flow-budget module in MODFLOW was used to track the amount of water flowing out of the wetted channel (constant-head cells) and into aquifer cells. We assumed that water that flows out of the wetted channel would flow back into the wetted channel at some downstream location and thus represents hyporheic exchange flow. A particle tracking postprocessing package, MODPATH [Pollock, 1994], was used to estimate HEF_{RT} at each well network site. The MODPATH requires a value for effective porosity, which ranges from 0.25 to 0.35 for sediment mixtures of boulders, gravel, and sand [Fetter, 1994]. We used the midrange value of 0.30. Wetted channels (constant-head cells) were used as starting points. Three particles were introduced to each stream cell in the Middle Lookout simulations, and nine particles were introduced to each stream cell in the simulations of other sites. Particles were tracked until they returned to the stream cells.

3.3. Sensitivity Analysis

[17] Models calibrated to the WS01 and Middle Lookout sites were also used in a sensitivity analysis to estimate the relative effect of each type of morphologic features on the development of the hyporheic zone. Thus geomorphic features were removed from the model simulations by adjusting the boundary conditions and rerunning the model to simulate subsurface flow without that particular type of feature. For example, to estimate the effect of pool-step sequences on hyporheic exchange flows in the WS01 site, pool-step sequences were removed by changing the head in the series of constant-head cells representing the stream surface to a smooth gradient, equaling the reach-averaged gradient measured at the WS01 well network site. To the extent possible, all other features were left unchanged. The sensitivity analysis examined the following geomorphic features: secondary channels, channel splits, pool-step or pool-riffle sequences, and sinuosity. For each model run, a flow-budget module and a particle tracking code were used to track changes in Q_{HEF} and HEF_{RT}, respectively. We assumed that the magnitude of change in both the Q_{HEF} and the HEF_{RT} indicates the relative importance of the particular feature to the development of the hyporheic zone.

[18] The sensitivity analysis was extended to analyze the full range in frequencies and sizes of channel morphologic features measured in the extensive stream surveys. We were concerned that the well network sites did not adequately characterize the range in variability of geomorphic features present among a wider selection of stream reaches and therefore did not represent the full range of influence that channel morphology can exert over the development of the hyporheic zone. Simplified models were constructed to characterize hypothetical stream reaches with average valley width, average saturated hydraulic conductivity, average aquifer thickness, and average wetted channel width measured from WS01 and Middle Lookout sites. These models

Table 2. Sizes and Frequency of Each Geomorphic Feature Used in the Simplified Stream Simulations in the Extended Sensitivity Analysis of Second-Order Streams and Fifth-Order Streams

Second-Order	Steps Gradient (m/m)/Number	Sinuosity, m/m	Secondary Channel	
			Length, m	Gradient, m/m
Maximum size	1.70/2	1.35	13.8	0.191
Average size	0.49/7	1.13	8.9	0.108
Minimum size	0.34/10	1.02	2.8	0.055

Fifth-Order	Riffles Gradient (m/m)/Number	Sinuosity, m/m	Secondary Channel		Channel Split	
			Length, m	Gradient, m/m	Length, m	Gradient, m/m
Maximum size	0.15/2	1.37	107.2	0.021	41	0.042
Average size	0.06/5	1.26	78.5	0.014	29.4	0.04
Minimum size	0.03/10	1.1	48.8	0.005	19.2	0.038

were used with the survey and map data collected from the RSLs in a series of simulation to analyze the influence of the minimum, average, and maximum sizes and numbers of each type of geomorphic features on hyporheic exchange flows.

[19] We were careful to balance the size and frequency of features as measured in stream surveys to provide realistic simulations. For example, surveys showed that steps had average gradients of 0.49 m/m in the WS01 study reach, but the largest and smallest steps had gradients of 1.70 and 0.2 m/m, respectively (Table 2). We created stream profiles in the simulation runs, spacing steps evenly along the stream reach and adjusting the total number of steps so that they would account for the average contribution of steps to elevation changes measured along the stream profiles (Table 3). In this example, use of the minimum size step would have result in fifteen 0.2 m/m steps. However, the maximum number of steps observed in a 50-m reach was only 10. Therefore ten 0.34 m/m steps were used in the simulation to examine the effects of minimum size steps.

[20] We developed model simulations to examine the observed range in (1) channel sinuosity, (2) the length of secondary channels, (3) the cross-valley gradient between secondary channels and the main stream, (4) the length of channel splits, (5) the cross-valley gradients between channel splits, and (6) the size and number of pool-step (or pool-riffle) sequences. Because secondary channels and channel splits in the second-order streams were not distinctive, we did not examine the effect of channel splits in the extended sensitivity analysis. Also, the influence of multiple morphologic features was not examined in the extended sensitivity analysis because simulating all possible combinations (minimum, mean, maximum) of all features measured was beyond the scope of the study. As before, we estimated Q_{HEF} for each model run and considered the differences in these values as indicators of the influence of the channel morphologic features analyzed. Because the analysis is based on survey data, the sensitivity analysis represents realistic limits on the development of hyporheic zones in mountain streams in response to individual channel morphologic features.

4. Results

4.1. Characteristics of Channel Morphology

[21] The WS01 and WS03 sites had similar channel morphology despite the difference in valley widths (Table 1). Channel gradients were steep, averaging 0.13 m/m at both sites, and pool-step sequences were frequent, with steps accounting for more than 50% of the elevation change along the longitudinal profile of the stream (Table 1). Steep steps (>0.15 m/m) were created where large logs or boulders blocked the stream, and sediment accumulated behind the logs. The boulders and logs that created steps also obstructed the channel, deflecting the stream so that the sinuosity was relatively high, averaging 1.3 m/m (Table 1). Several secondary channels were present in each stream reach, but these were always short and located close to the main channel. The extended survey of the study reaches showed that the well network sites reasonably represent the extended study reaches (Table 3), except that sinuosity, the number of steps, and the contribution of steps to change in elevation were higher in the portion of the reach covered by the well networks.

[22] The channel morphology of the unconstrained Middle Lookout site was different from the Bedrock-constrained site. The active channel in the Middle Lookout site was nearly 3 times wider than the Bedrock-constrained site, and the channel sinuosity was correspondingly greater (Table 1). Secondary channels and channel splits around gravel bars and islands were present in the Middle Lookout site, whereas these features were lacking at the Bedrock-constrained site. Further, the wide active valley floor permitted development of relatively long secondary channels that were located well away from the main channel (Figure 1).

Table 3. Morphologic Characteristics of Extended Survey Reaches

	WS01	WS03	Middle Lookout	Bedrock Constrained
Stream discharge, L/s	3	4	720	720
Reach length, m	200	250	1500	350
Number of RSLs	6	7	8	2
Channel width, m	1.8	1.8	8.6	8.7
Valley width, m	14.8	7.9	38.7	16.8
Channel gradient, m/m	0.13	0.13	0.02	0.01
Sinuosity, m/m	1.1	1.1	1.3	1.1
Number of steps/riffles per 100 m	11.1	8.4	2.1	0.9
Contribution of steps/riffles to change in elevation, %	51.0	53.9	50.3	39.7
Elevation changes resulting from steps/riffles, m/100 m	6.6	7.0	1.0	0.4

Table 4. Secondary Channels and Channel Splits at Each Study Site

	WS01 and WS03	Middle Lookout
Number of secondary channels	6	6
Length, m	7.9	78.5
Gradient, m/m	0.10	0.01
Number of channel splits	4	3
Length, m	3.1	29.4
Gradient, m/m	0.04	0.04

The Middle Lookout site also had a steeper longitudinal gradient, and the frequency of pool-riffle sequences was greater (Table 1).

[23] In general, the geomorphic attributes measured along the extended survey of fifth-order reaches were similar to those observed in the well network sites (Tables 1 and 3). The largest difference was in the relative amount of elevation change in the stream channel resulting from pool-riffle sequences, which were more important in the well network sites. Secondary channels were common in the unconstrained reach, where six out of 10 meander bars were backed by such channels. In all cases, surface water elevations in the secondary channels were lower than in the main channel, creating relatively gentle cross-valley head gradients. In comparison, channel splits created much steeper cross-valley gradients but were both shorter and less frequent than secondary channels (Table 4). We did not observe secondary channels or channel splits in the Bedrock-constrained reach; however, only two RSLs were surveyed in this reach, in comparison to eight RSLs in Middle Lookout reach.

4.2. Hyporheic Exchange Flows at Well Network Sites

[24] After the initial MODFLOW simulations, we compared the simulated water table and the observed water table at each well location. Where simulated and observed values showed large differences, hydraulic conductivities were adjusted around those wells to match the simulated and observed water tables. The final calibrated models had mean head residuals less than 0.1 m in the second-order stream sites and less than 0.2 m in the fifth-order stream sites, suggesting that the simulation of the hyporheic exchange flow in the study sites was realistic.

4.2.1. Exchange Flow Paths and the Extent of the Hyporheic Zone

[25] The MODFLOW simulations showed that the hyporheic zone extent was similar in the unconstrained WS01 and constrained WS03 sites. The equipotential lines of the well network sites showed that hyporheic flow paths extended laterally around step-pool sequences and appeared to be the primary features driving hyporheic exchange (Figure 2). In general, these hyporheic flow paths tended to be short or quickly captured by strong, down-valley trending flow paths. Exchange flows around steps were most obvious at the largest steps, where the vertical change in hydraulic head across the pool-step sequence was greatest. In both WS01 and WS03, the largest steps were created by large logs. Secondary channels appeared to have limited influence on the development of hyporheic zones in these small streams because the secondary channels were always located close to the main channel.

[26] The well network in the unconstrained fifth-order stream site was restricted to the active channel, where it was possible to reach the water table with hand-driven wells. Model simulations showed that hyporheic exchange flows were present throughout the active channel area. Of course, the hyporheic zone may have extended beyond the active channel in some places, but without wells, we cannot determine the limits of its lateral extent.

[27] MODFLOW simulations showed that exchange flows between the main channel and secondary channel appeared to dominate the hyporheic zone (Figure 1). In this location, exchange flow paths exceeded 30 m in length and were oriented ~45° to the valley axis. The MODFLOW simulations indicated that the steepest head gradients were through the island bar that was present between the split channels at the downstream end of the study site. Steep riffles located at the head of the island bar in the right channel and near the tail of the bar in the left channel create steep head gradients between the two channels (Figure 3). Pool-riffle sequences had little effect on exchange flows, except at the steep riffle at the junction of McRae and Lookout Creeks (Figure 1). Overall, hyporheic flow paths identified from MODFLOW simulations tended to be long and often flowed laterally across the floodplain, from the main channel toward secondary channels.

[28] The size of the hyporheic zone was small in the Bedrock-constrained site, where bedrock limits the extent of the near-stream aquifer to a narrow gravel bar along the length of the left bank (Figure 1). Groundwater discharge from springs located along the valley margin at the head of the gravel bar limited the penetration of stream water into the subsurface, further restricting the extent of the hyporheic zone. The pool-riffle sequences located near the head and middle of the gravel bar were the primary geomorphic features driving hyporheic exchange in the Bedrock-constrained site.

4.2.2. Q_{HEF} and the Effects of Channel Morphology

[29] Hyporheic exchange flow (Q_{HEF}) was estimated from the calibrated model runs using MODFLOW's flow budget feature. Estimates suggest that Q_{HEF}, normalized to the length of the stream, was greatest at the Middle Lookout
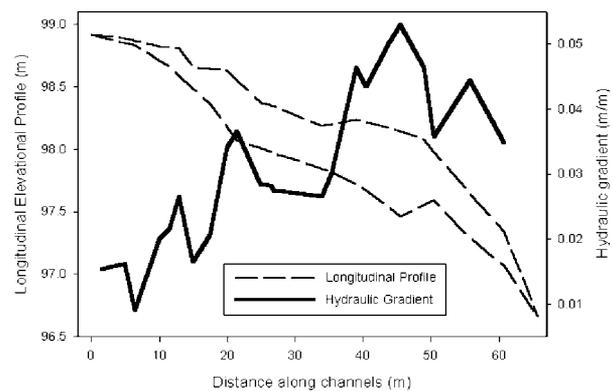

Figure 3. Longitudinal profiles of stream water elevations for the right and left stream channels at the channel split in the middle Lookout Creek study site. Bold line shows head gradient, through the island gravel bar separating the two channels.

site, and by comparison, quite small at the other three sites (Figure 4). However, these comparisons are often confounded by differences in stream size. Stream size is most often expressed in terms of stream discharge but can also be expressed in terms of streambed area. Normalizing Q_{HEF} by streambed area showed that the amount of hyporheic exchange flow relative to streambed area was largest in Middle Lookout, the unconstrained fifth-order stream site, intermediate in the second-order stream sites, and lowest in the Bedrock-constrained site (Figure 4). Normalizing Q_{HEF} by stream discharge shows that the amount of hyporheic exchange flow relative to stream discharge was much larger in the second-order stream sites than in the fifth-order stream sites. We estimate that approximately 76% of stream discharge in WS01, and more than 100% of stream discharge in WS03, would flow through the hyporheic zone in a 100-m reach (Figure 4). Only 5% and 0.6% of the stream discharge was exchanged with the subsurface in the unconstrained and constrained fifth-order sites, respectively (Figure 4).

[30] We further analyzed the influence of channel morphologic features on hyporheic exchange flows at the unconstrained secnd- and fifth-order stream study sites using a sensitivity analysis in which we eliminated each type of morphologic feature in turn from the calibrated models and recalculating Q_{HEF} for each model run. The constrained fifth-order study site lacked most of these features, and there
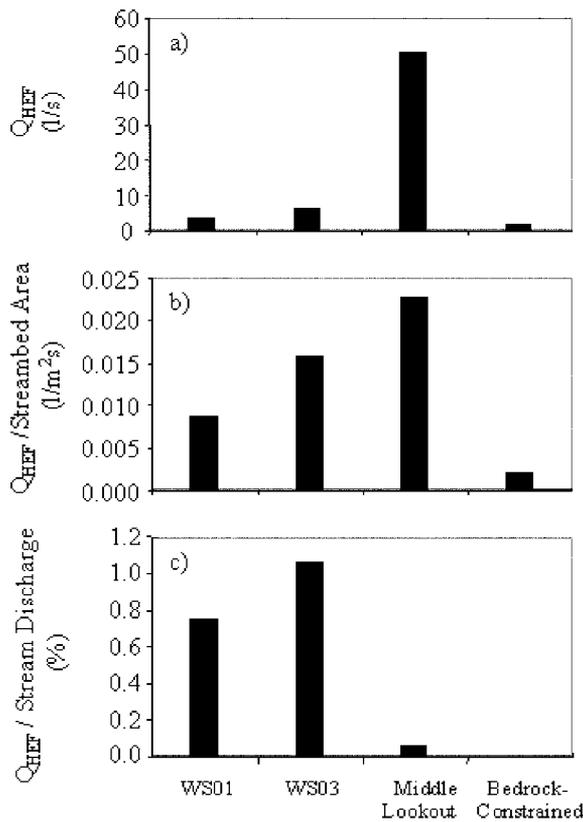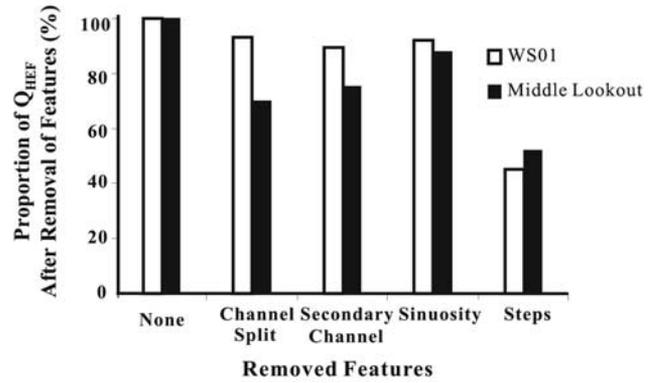

Figure 5. Comparison of predicted changes in hyporheic exchange flow (Q_{HEF} in l/s) following the removal of classes of channel morphologic features from MODFLOW simulations for WS01 and Middle Lookout Creek. Changes in Q_{HEF} are expressed as a percentage from the original, best-fit model simulation.

were little differences in morphological characteristics between the constrained and unconstrained second-order sites, so the analysis focused on the unconstrained study sites in both stream sizes.

[31] Removal of the secondary channel, the channel split, and channel sinuosity had very little influences on Q_{HEF} at the WS01 site (Figure 5). However, removal of the pool-step sequence reduced Q_{HEF} by 54% in WS01. At the Middle Lookout site, removal of the secondary channel reduced Q_{HEF} by 25%, removal of the channel split reduced Q_{HEF} by 30%, and removing sinuosity reduced Q_{HEF} by 12% (Figure 5). The greater importance of these features in the unconstrained fifth-order site, relative to the second-order site, was expected given the influence of these morphologic features on hyporheic flow paths observed from equipotentials of the water table surface (Figures 1 and 2). However, removal of pool-riffle sequences at the Middle Lookout site had the greatest influence on Q_{HEF}, reducing flows by 48% (Figure 5), despite their apparently minimal influence in shaping the horizontal extent of the hyporheic zone (Figure 1).

4.2.3. HEF$_{RT}$ and the Effects of Channel Morphology

[32] We estimated the residence time distribution of stream water in the hyporheic zone (HEF$_{RT}$) using MODPATH. In general, the estimates of HEF$_{RT}$ showed that exchange flows were dominated by short residence-time exchanges, but there were important differences among sites (Figure 6). The peak of the frequency distribution was between 2 and 4 hours in the Middle Lookout site, with a median residence time of 27 hours. HEF$_{RT}$ also peaked between 2 and 4 hours in both WS01 and WS03, and the two second-order sites had similar median residence times of 18 hours. Residence times were much longer at the Bedrock-constrained site, with the peak of the frequency distribution occurring between 13 and 22 hours and a median residence time of 214 hours. In general, HEF$_{RT}$ tended to be more dominated by short residence time flow paths in the second-order streams than in fifth-order streams, as might be expected from the relatively high head gradients and the limited areal extent of the hyporheic zone in these steep headwater streams.
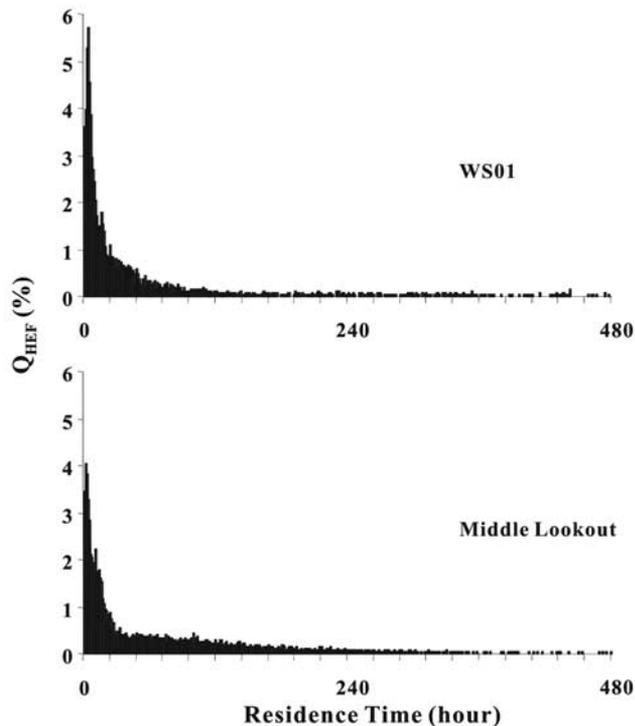

Figure 4. Amount of hyporheic exchange flow predicted from MODFLOW simulations of each study site, (a) normalized to 100-m channel length (Q_{HEF}), (b) normalized to streambed area (Q_{HEF}:A), and (c) normalized to stream discharge (Q_{HEF}:Q).

Figure 6. Residence time distributions of hyporheic exchange flows (HEF$_{RT}$) estimated using the particle-tracking routine in MODPATH, for (a) WS01 and for (b) Middle Lookout Creek. Residence times are shown as a percentage of the total, to facilitate comparisons between sites.

[33] We analyzed the relative influence of channel morphologic features on HEF$_{RT}$ at the unconstrained study sites by eliminating morphologic features from our calibrated models and recalculating HEF$_{RT}$ for each model run. The difference in HEF$_{RT}$ was compared by subtracting one frequency distribution from another. Removal of steps from WS01 model reduced exchange flows with residence times <24 hours and increased the relative proportion of exchange flows with residence times between 24 and 141 hours (Figure 7). Removal of other types of geomorphic features from the second-order stream simulations did not show clear effects on HEF$_{RT}$.

[34] Removal of riffles from the Middle Lookout simulation had the largest effect on HEF$_{RT}$, again reducing exchange flows with residence times <24 hours, and increasing the relative importance of longer residence time exchange flows (Figure 8). The effect of removing the channel split was similar to that of removing riffles, whereas removal of the secondary channel had a nearly opposite effect in the Middle Lookout site. The effect of removing channel sinuosity consistently increased the relative proportion of long residence time flow paths (Figure 8).

4.3. Model Simulations of Simplified Streams

[35] The sensitivity analysis was extended to include a fuller range of size and frequencies of morphologic features measured in our extended stream surveys (Table 3). Results from the simulation of the second-order stream showed that pool-step sequences drove more hyporheic exchange flow

(0.22−0.54 L/s) than did any other feature (Figure 9). Step size was also important, with two of the largest-sized steps driving more hyporheic exchange flow within a reach than did numerous, but smaller-sized steps, even though the smaller steps accounted for the same total elevation change along the longitudinal profile of the reach. The influence of pool-step sequences clearly dominated hyporheic exchange flow in second-order streams, with even the series of 10 small steps resulting in more hyporheic exchange than resulted from the maximum expression on any other morphologic feature.

[36] The sensitivity analysis showed that pool-riffle sequences were also the largest drivers of hyporheic exchange flows in fifth-order streams (Figure 9). The longitudinal gradient of the riffles influenced Q$_{HEF}$ at the reach scale such that two riffles with 0.15 m/m gradients resulted in 3 times more hyporheic exchange flow than 10 riffles with 0.03 m/m gradients. The effect of other morphologic features was relatively more important in fifth-order streams than in the second-order stream. The maximum expression of channel splits, secondary channels, and sinuosity (Table 2) all resulted in more Q$_{HEF}$ within the stream reach than did a series of 10 of the lowest-gradient riffles (Figure 9).

5. Discussion

5.1. Use of Groundwater Flow Models in Hyporheic Studies

[37] Combining fine-scale surveys of surface-visible morphologic features with MODFLOW simulations was an effective way to investigate hyporheic exchange flows in the mountain streams studied. A few previous studies have used two-dimensional numerical groundwater-flow models to investigate stream-subsurface water interactions within well-defined study sites where hydrologic information was available from well networks [*Harvey and Bencala*, 1993; *Wondzell and Swanson*, 1996a; *Wroblicky et al.*, 1998]. In this study, the use of groundwater-flow models was extended with a sensitivity analysis to isolate and examine the relative influence of specific morphologic features in morphologically complex stream reaches. This approach allowed us to examine a wide range of physical stream conditions, and to do so much more quickly, than would have been possible with direct empirical studies.

[38] Numerical groundwater flow models have limitations, however. First, models are data intensive. Groundwater-flow models require spatially distributed inputs of saturated hydraulic conductivity (K), and boundary conditions need to be defined along the margins of the model domain. These data can be collected from a well network; however, the data are specific to the particular well network and stream reach studied. Consequently, these models are not readily transferable to other streams. Second, models are difficult to verify. The boundary conditions and both the value and spatial distribution of K are difficult to measure and the resulting models may not be unique. That is, several different combinations of boundary conditions and saturated hydraulic conductivity can provide equally good fits to the water table elevations observed in the well networks. However, some predictions of groundwater simulations are more easily verified than others. For example, the predicted hyporheic flow paths agreed with the movement of a NaCl
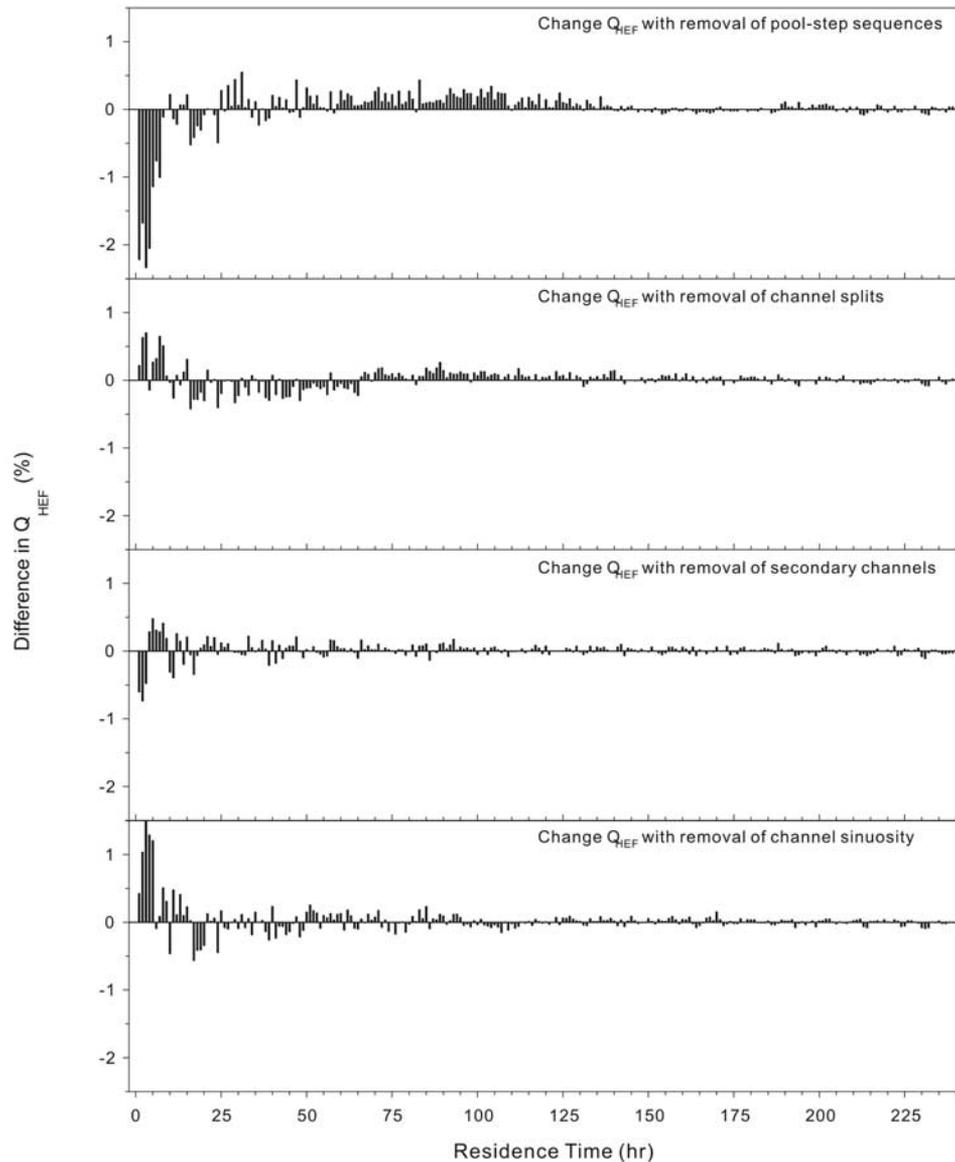
Figure 7. Changes in residence time distributions (HEF$_{RT}$) following the removal of (a) pool-step sequences, (b) channel splits, (c) secondary channels, and (d) channel sinuosity from MODFLOW simulations of the WS01 site. Negative values denote a decrease in the frequency of exchange flows with a given residence time, relative to that predicted from the original, best-fit model simulation.

tracer injected into a well at both the WS01 and Middle Lookout Creek sites (T. Kasahara and S. Wondzell, unpublished data, 1999). In contrast, Q_{HEF} and HEF$_{RT}$ are more difficult to verify, because they are strongly dependent on the saturated hydraulic conductivity, which is difficult to measure [*Freeze and Cherry*, 1979]. Estimates of K from slug tests are uncertain [*Hyder and Butler*, 1995], and the estimates apply only to a small region surrounding each well. We attempted to confirm the results of our slug tests using well tracer injections in WS01 and in Middle Lookout Creek. Estimates of K, made from the tracer injections (0.01 cm/s in WS01; 0.50 cm/s in Middle Lookout Creek), agree with the geometric mean of K estimated from slug tests on wells in the part of the study site that the well tracer injection was conducted (0.02 cm/s in WS01; 0.10 cm/s in Middle Lookout Creek). Also, the models were hetero-

geneous, with the horizontal variation in K based on slug tests from each well in the well networks, which increased the realism of the simulations, although at a relatively coarse grain because of the spacing of the wells. The tracer injection results suggested that the values of K used in models were realistic and captured horizontal variation in aquifer properties at a spatial scale of several to tens of meters.

[39] Although our MODFLOW simulations were three-dimensional, in that we utilized multiple layers, the models are based on a simplified description of the vertical flow of water. The data used to parameterize the models, to establish both initial condition and boundary conditions, and to calibrate the models were measured from our well network. However, we were unable to install vertically nested piezometers to measure the vertical heterogeneity in saturated
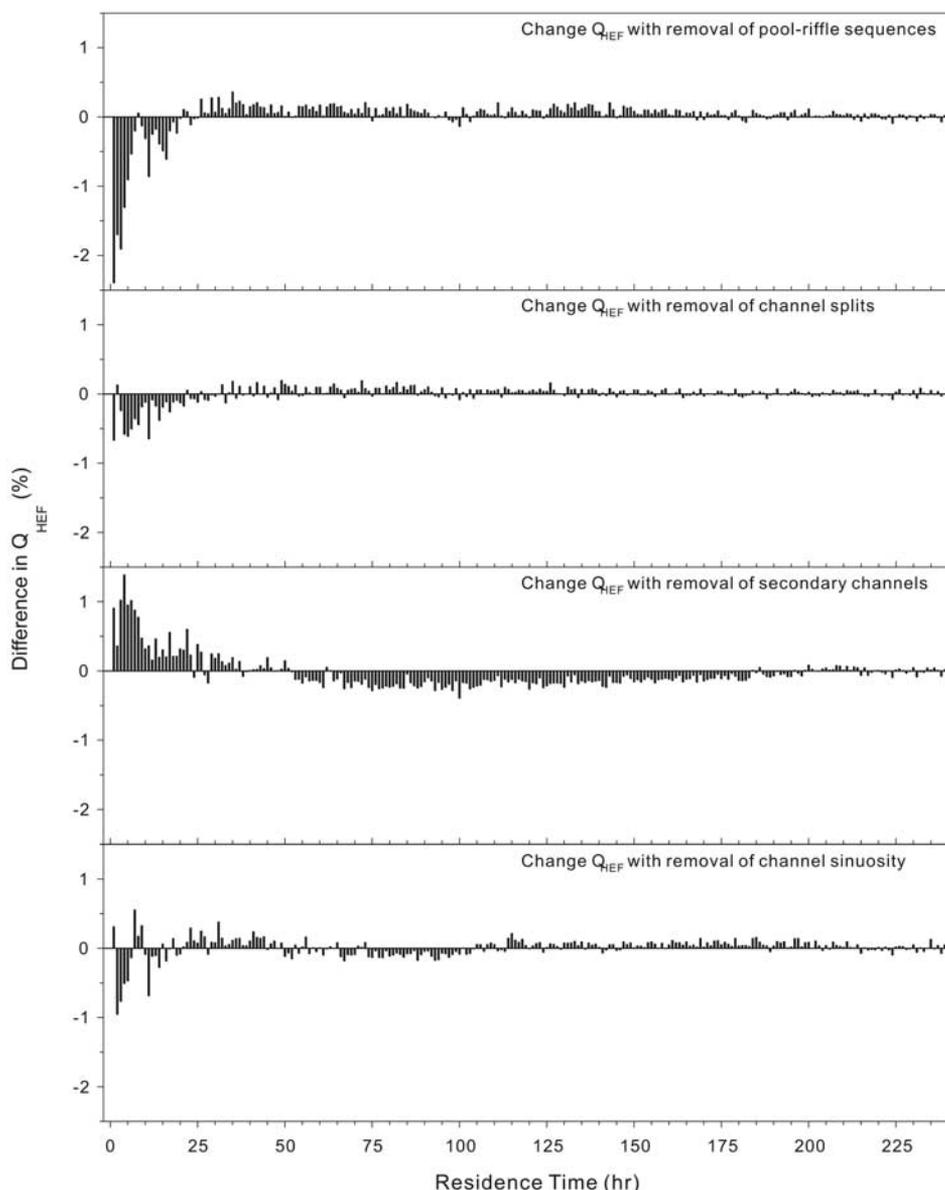
Figure 8. Changes in residence time distributions (HEF$_{RT}$) following the removal of (a) pool-step sequences, (b) channel splits, (c) secondary channels, and (d) channel sinuosity from MODFLOW simulations of the Middle Lookout site. Negative values denote a decrease in the frequency of exchange flows with a given residence time, relative to that predicted from the original, best-fit model simulation.

hydraulic conductivity. Therefore the data from which the models are derived are essentially two-dimensional. Also, the depth of valley alluvium (aquifer thickness) and the variation in depth both across the width and along the length of the valley are unknown, requiring assumptions that further simplify the simulation of the vertical component of water flow within the aquifer.

[40] The size of morphologic features that can be included in numerical groundwater-flow models is determined by the size of the cells used in the model and the size of the model domain. For example, the models constructed for the second-order streams studied used 0.3 × 0.3 m cells, and morphologic features smaller than the cell size cannot be included in the simulations. Several studies have shown that small-scale morphologic features can drive hyporheic

exchange flow [*Thibodeaux and Boyle*, 1987; *Elliott and Brooks*, 1997]. This study, however, did not incorporate the influence of small-scale features because of practical limits on the minimum size of cells that can be used in the simulations. Similarly, the size of the Middle Lookout model domain was about 75 × 170 m, and hyporheic exchange occurring at larger scales, such as those shown by *Hinkle et al.* [2001] or *Baxter and Hauer* [2000], cannot be simulated. Our simulations included morphologic features at a wide range of spatial scales that can drive hyporheic exchange flow. The effects of some potentially important morphologic features, however, at both the smallest and largest scales, could not be investigated.

[41] Regardless of the limitations mentioned above, numerical groundwater flow models offer several advan-
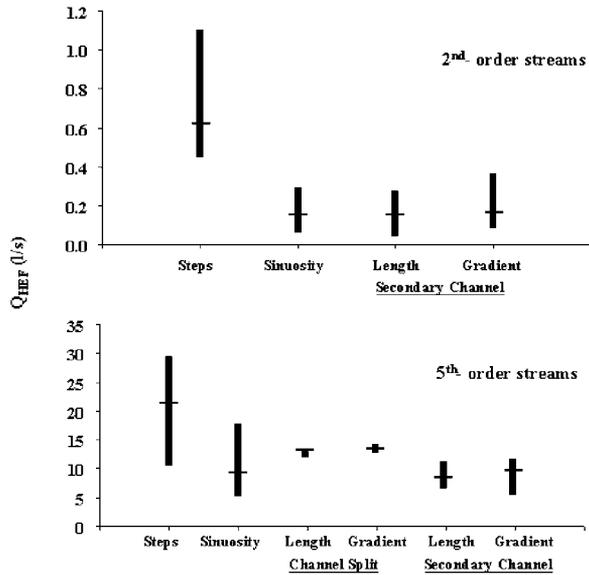
Figure 9. Sensitivity of hyporheic exchange flows (Q_{HEF}) to the size and number of pool-step or pool-riffle sequences, amount of channel sinuosity, the length and cross-island-bar gradients of channel splits, and length and cross-valley gradients of secondary channels predicted from simplified MODFLOW simulations of (a) the WS01 site and (b) the Middle Lookout Creek site. The maximum and minimum expression of each type of morphologic feature was determined from stream surveys.

tages for examining hyporheic zones. First, the size of both the model domain and model cells can be varied so as to allow hyporheic investigations across a range of spatial scales, from a single channel unit to long stream reaches, depending on the focus of a study. Second, sensitivity analysis can be used to examine the influence of the geomorphic setting on hyporheic exchange, examining the influence of factors such as depth of alluvial sediment, valley-floor width, or variations in saturated hydraulic conductivity. Third, sensitivity analysis can be used to isolate individual channel-unit scale features from the overall reach-scale response. Fourth, the modeling packages are designed to support three-dimensional simulations and thus can simulate both horizontal and vertical components of hyporheic exchange flows. Finally, and perhaps most important, groundwater flow models are physically based, mechanistic simulations from which flow and residence time can be quantified. Thus we believe that the advantages of using numerical groundwater flow models outweigh the disadvantages.

5.2. Effects of Channel Morphology on the Hyporheic Zone

5.2.1. Effects on Hyporheic Exchange Flow

[42] The results clearly document the strong driving force that channel morphologic features exert on hyporheic exchange flow and support previous studies that have identified the importance of specific morphologic features [*Harvey and Bencala*, 1993; *Wondzell and Swanson*, 1996a; *Fernald et al.*, 2001]. However, the ways in which valley-

floor and channel morphology controlled exchange flow differed between the second- and fifth-order streams. This difference in geomorphic control is explained by the dissimilarity in channel morphology between the two sizes of streams. Hyporheic exchange flows were dominantly controlled by pool-step sequences in the steep channels of the second-order streams. In contrast, low gradients and wide valley floors provided space for fluvial processes to build complex channel morphologies with high sinuosity, frequent secondary channels, channel splits and island bars, as well as pool-riffle sequences in the unconstrained fifth-order reach. Unlike second-order streams, longitudinal gradients were gentle so that hyporheic exchange flows were strongly influenced by the full suite of morphologic features present.

[43] The second- and fifth-order streams differed in the degree to which channel constraint influenced hyporheic exchange flows. Even though the constrained fifth-order stream had a longitudinal gradient similar to that of the unconstrained fifth-order stream, the narrow valley floor, bounded by bedrock walls, limits the space available for fluvial processes to build morphologically complex channels. Therefore there were large differences between the two fifth-order stream reaches studied, and hyporheic exchange flows were sensitive to these differences. That was not the case in the steep, second-order streams where channel constraint did not appear to influence the development of the hyporheic zone.

[44] Hyporheic exchange flows in the second-order streams studied were primarily driven by pool-step sequences, in both the constrained and unconstrained reaches. The influence of steps was apparent in the flow paths drawn from contour maps of water table elevations (Figure 2), in the amounts of Q_{HEF} (Figure 5) and HEF$_{RT}$ (Figure 7) estimated from model simulations, and in the sensitivity analysis (Figure 9). The lack of a difference between the constrained and unconstrained streams appears to result from the steepness of the longitudinal gradients. Steep channel gradients in the second-order streams resulted in the presence of numerous step-pool sequences (Table 3) and prevented the development of extensive secondary channels (Table 4). Channel sinuosity was relatively high in both second-order reaches because boulders and logs obstructed and diverted the stream channel. Even so, the steep, down-valley head gradients prevented development of a strong lateral component in subsurface flows. Consequently, channel morphologies exerted similar influence on the hyporheic zone, despite the differences in channel constraint between the two reaches.

[45] Inspection of the contour maps of water table elevations generated from the MODFLOW simulation (Figure 1), and from contour maps produced by kriging elevations observed directly from the well network [see *Wondzell and Swanson*, 1999, Figure 8], show that secondary channels control the location and direction of flow paths through the hyporheic zone in the unconstrained fifth-order stream. Previous research at this study site [*Wondzell and Swanson*, 1999], and studies by *Stanford et al.* [1994], *Wondzell and Swanson* [1996a], and *Poole* [2000], all showed the strong influence that secondary channels exert on hyporheic exchange flows in wide, alluvial reaches of mountain rivers. However, our model simulations and subsequent sensitivity

analysis showed that removal of riffles reduced Q_{HEF} by approximately 50%, whereas removal of secondary channels reduced Q_{HEF} by only 25% (Figure 5).

[46] The unexpected importance of pool-riffle sequences in the unconstrained fifth-order stream reach can be explained by considering interactions among morphologic features. Cross-valley hydraulic gradients between main stem and secondary channels, or between split channels, can be created by pool-riffle sequences. Stream water elevations in one channel will drop steeply through a riffle, creating a cross-valley head gradient between the channels that will be maintained for some distance (Figure 3). Differences in overall longitudinal gradients between two channels can also create cross-valley head gradients. Thus hyporheic exchange flows initiated where pool-riffle sequences create steep, local head gradients can be captured by cross-valley flows between the main and secondary channel. These interactions between pool-riffle sequences and secondary (or split) channels tend to increase cross-valley gradients and enhance hyporheic exchange. The large decrease in Q_{HEF} observed after the removal of pool-riffle sequences resulted not only from the absence of pool-riffle sequences but also from the reduction in influence of secondary channels. These results indicate substantial interactive effects among morphologic features and that the effects of multiple morphologic features can be complementary.

[47] The differences observed in this study between small and large streams and between constrained and unconstrained streams would not necessarily occur in other geomorphic settings. For example, in landscapes where headwater streams are characterized by wider valley floors and gentler longitudinal gradients, we would expect a greater complexity of morphologic features, which would produce hyporheic exchange flows similar to those observed in the unconstrained, fifth-order stream reach. Conversely, in landscapes where low-gradient, unconstrained streams flow over fine-textured sediment, the influence of cross-valley channel complexity on hyporheic exchange flow would be greatly reduced.

5.2.2. Effects on Hyporheic Residence Time Distributions

[48] Hyporheic residence time is determined by a combination of saturated hydraulic conductivity, head gradient, and flow path length. The relatively short hyporheic flow paths around steps and riffles, or between channel splits, combined with coarse-textured alluvium resulted in relatively short residence time distributions for hyporheic exchange flows driven by these features. In contrast, flow path lengths between main stem and secondary channels in the fifth-order, unconstrained reach tended to be long and were driven by relatively shallow head gradients, so that residence time distribution was long. Thus different types of geomorphic features create hyporheic exchange flows with different residence time distributions.

[49] The hyporheic zone contained relatively more, short-residence-time exchange flows in the second-order stream sites, than in the fifth-order sites, because of the dominance of step-pool sequences in driving exchange flow. The Middle Lookout site had relatively more long-residence-time exchange flows because the secondary channel drove abundant cross-valley flows. However, short-residence-time

exchanges were also well represented because of several pool-riffle sequences and because of the channel split (Figures 6 and 8).

[50] The longest residence time distribution was in the Bedrock-constrained site (fifth-order). A relatively long, low-gradient channel unit called a "glide" extends most of the length of the Bedrock-constrained site. Pool-riffle sequences were rare, so that hyporheic flow paths tend to parallel the stream, flowing the length of the narrow gravel bar. Longitudinal head gradients along this portion of the reach were low, and average saturated hydraulic conductivity was also low. Consequently, subsurface flow velocities were slow and many of the hyporheic flow paths were quite long, even though the channel is tightly constrained.

5.3. Influence of the Hyporheic Zone on Stream Ecosystem Properties

[51] Interest in the effect of the hyporheic zone on a variety of physical, chemical, and biological stream processes often uses a "mass budget" perspective, focusing on situations where the influence of the hyporheic zone on nutrient cycling or stream water temperature is determined by the amount of hyporheic exchange flow occurring within a stream reach. Hyporheic exchange flow can be expressed as a ratio of Q_{HEF} to stream discharge ($Q_{HEF}:Q$), and it is expected that the greatest potential for hyporheic exchange flows to influence stream ecosystem processes will be in reaches with high $Q_{HEF}:Q$ ratios [*Findlay*, 1995; *Valett et al.*, 1996].

[52] In the stream reaches studied, the $Q_{HEF}:Q$ ratio was much larger in the second-order stream sites than in the fifth-order stream sites. The simulations predict that 76% of stream discharge in WS01, and more than 100% of stream discharge in WS03, would flow through the hyporheic zone in a 100-m reach, and corresponding turnover lengths of stream water through the hyporheic zone would be 132 m in WS01 and 94 m in WS03 at summer low flow. Only 5% of the stream discharge was exchanged with the subsurface in the unconstrained fifth-order site, giving a turnover length of 1.69 km. The estimated turnover length was 20 km at the constrained fifth-order site, where exchange flows, relative to stream discharge, accounted for only 0.6% of stream discharge per 100 m at summer low flow. Thus the smaller streams had higher proportions of stream water flowing through the hyporheic zone, suggesting that the hyporheic zone in the second-order streams has a greater potential to influence stream ecosystems. Such comparisons give the impression that hyporheic exchange flow is consistently more important in smaller streams than in larger streams. However, calculating reach-scale mass budgets hides smaller-scale patterns that may have important effects on stream-ecosystem processes.

[53] Some biological and chemical processes in streams occur preferentially at the stream water-sediment interface. For example, many studies have shown that the hyporheic zone can be an important source of nitrogen in nitrogen-limited streams [*Triska et al.*, 1989; *Holmes et al.*, 1994; *Jones et al.*, 1995; *Wondzell and Swanson*, 1996b], and a previous study reported higher algal production at upwelling sites than at downwelling sites [*Valett et al.*, 1990]. If streambed algae (periphyton) immobilize the nitrogen available in return flows of hyporheic water as it passes

through the streambed, these nutrients will not be mixed into the overlying water column. In this case, the ratio of hyporheic exchange flow to streambed area (Q_{HEF}:A) is likely to be a better measure of the relative importance of the hyporheic zone in stream ecosystem processes. For the stream reaches we studied, the Q_{HEF}: A ratio was largest in the Middle Lookout site, intermediate in the second-order stream sites, and lowest in the Bedrock-constrained site (Figure 4). This suggests that hyporheic exchange may have a greater potential to influence stream ecosystem processes in the larger mountain streams than in the smaller streams.

6. Conclusions

[54] Surface-visible valley-floor and channel morphologic features strongly control hyporheic exchange flow, and these controls differed with stream size and channel constraint in four mountain stream reaches. These differences reflect the dissimilarity of channel morphology among the streams that control both the amount and residence time of hyporheic exchange flows.

[55] The methods employed in this study are readily transferable to other locations, helped by the ready availability of software packages, training courses, and model documentation for running groundwater flow models. We believe that these techniques should be employed elsewhere to build a stronger, physically based understanding of the factors controlling hyporheic exchange flows, to quantify both the amount and residence time distributions of those exchange flows, and to build the fundamental understanding of hydrological processes to allow more thorough evaluation of the relative importance of the hyporheic zone in stream ecosystem processes.

[56] Further research on the relationships between channel morphology and hyporheic exchange flows will provide valuable insights into the role of the hyporheic zone in stream networks in different geomorphic settings. Quantifying the role of channel morphologic features on hyporheic exchange flow sets the stage to frame the subsurface flow systems of floodplains in a geomorphic context that will facilitate comparisons among drainage basins in different geomorphic settings.

References

Anderson, M. P., and W. W. Woessner, *Applied Groundwater Modeling*, Academic, San Diego, Calif., 1992.

Baxter, C. V., and F. R. Hauer, Geomorphology, hyporheic exchange, and selection of spawning habitat by bull trout (*Salvelinus confluentus*), *Can. J. Fish. Aquat. Sci.*, 57, 1470–1481, 2000.

Bierlmaier, F. A., and A. McKee, Climatic summaries and documentation for the primary meteorological station, H. J. Andrews Experimental Forest, 1972 to 1984, U.S. Dep. of Agric. For. Serv., Portland, Oreg., 1989.

Bouwer, H., and R. C. Rice, A slug test for determining hydraulic conductivity of unconfined aquifers with completely or partially penetrating wells, *Water Resour. Res.*, 12, 423–428, 1976.

Elliott, A. H., and N. H. Brooks, Transfer of non-sorbing solutes to a streambed with bed forms: Laboratory experiments, *Water Resour. Res.*, 33, 137–151, 1997.

Engineering Computer Graphic Laboratory of Brigham Young University, *Groundwater Modeling System v2.1 Reference Manual*, Provo, Utah, 1998.

Fernald, A. G., P. J. Wigington, Jr., and D. H. Landers, Transient storage and hyporheic flow along the Willamette River: Field measurement and model estimates, *Water Resour. Res.*, 37, 1681–1694, 2001.

Fetter, C. W., *Applied Hydrogeology*, Prentice-Hall, Upper Saddle River, N. J., 1994.

Findlay, S., Importance of surface-subsurface exchange in stream ecosystems: The hyporheic zone, *Limnol. Oceanogr.*, 40, 159–164, 1995.

Freeze, R. A., and J. A. Cherry, *Groundwater*, Prentice-Hall, Upper Saddle River, N. J., 1979.

Grimm, N. B., and S. G. Fisher, Exchange between interstitial and surface water: Implications for stream metabolism and nutrient cycling, *Hydrobiologia*, 111, 219–228, 1984.

Harvey, J. W., and K. E. Bencala, The effect of streambed topography on surface-subsurface water exchange in mountain catchments, *Water Resour. Res.*, 29, 89–98, 1993.

Hill, A. R., C. F. Labadia, and K. Sanmugadas, Hyporheic zone hydrology and nitrate dynamics in relation to the streambed topography of a N-rich stream, *Biogeochemistry*, 42, 285–310, 1998.

Hinkle, S. R., J. H. Duff, F. J. Triska, A. Laenen, E. B. Gates, K. E. Bencala, D. A. Wentz, and S. R. Silva, Linking hyporheic flow and nitrogen cycling near the Willamette River—A large river in Oregon, USA, *J. Hydrol.*, 244, 157–180, 2001.

Holmes, R. M., S. G. Fisher, and N. B. Grimm, Parafluvial nitrogen dynamics in a desert stream ecosystem, *J. N. Am. Benthol. Soc.*, 13, 468–478, 1994.

Holmes, R. M., J. B. Jones, S. G. Fisher, and N. B. Grimm, Denitrification in a nitrogen-limited stream ecosystem, *Biogeochemistry*, 33, 125–146, 1996.

Hyder, Z., and J. J. Butler, Jr., Slug tests in unconfined formations: An assessment of the Bouwer and Rice Technique, *Ground Water*, 33, 16–22, 1995.

Jones, J. B., S. G. Fisher, and N. B. Grimm, Nitrification in the hyporheic zone of a desert stream ecosystem, *J. N. Am. Benthol. Soc.*, 14, 249–258, 1995.

Kaplan, L. A., and J. D. Newbold, Surface and subsurface dissolved organic carbon, in Streams and Ground Waters, edited by J. A. Jones and P. J. Mulholland, pp. 237–258, Academic, San Diego, Calif., 2000.

McDonald, M. G., and A. W. Harbaugh, A modular three-dimensional finite difference groundwater flow model, *OR-83-875*, U.S. Geol. Surv., Reston, Va., 1988.

Mulholland, J. L., J. L. Tank, D. M. Sanzone, W. M. Wollheim, B. J. Peterson, J. R. Webster, and J. L. Meyer, Nitrogen cycling in a forest stream determined by a 15N tracer addition, *Ecol. Monogr.*, 70, 471–493, 2000.

Pollock, D. W., User's guide for MODPATH/MODPATH-PLOT, version 3, A particle tracking post-processing package for MODFLOW, the U.S. Geological Survey finite-difference ground-water flow model, U.S. Geol. Surv., Reston, Va., 1994.

Poole, G. C., Analysis and dynamic simulation of morphologic controls on surface- and ground-water flux in a large alluvial flood plain, Ph.D. dissertation, Univ. of Mont., Missoula, 2000.

Stanford, J. A., and J. V. Ward, The hyporheic habitat of river ecosystems, *Nature*, 335, 64–66, 1988.

Stanford, J. A., and J. V. Ward, An ecosystem perspective of alluvial rivers: Connectivity and the hyporheic corridor, *J. N. Am. Benthol. Soc.*, 12, 48–60, 1993.

Stanford, J. A., J. V. Ward, and B. K. Ellis, Ecology of the alluvial aquifers of the Flathead River, Montana, in *Groundwater Ecology*, edited by J. Gibert, D. L. Danielopol, and J. A. Stanford, pp. 367–390, Academic, San Diego, Calif., 1994.

Stoertz, M. W., and K. R. Bradbury, Mapping recharge areas using a ground-water flow model—A case study, *Groundwater*, 27, 220–228, 1989.

Thibodeaux, L. J., and J. O. Boyle, Bed-form generated convective transport in bottom sediment, *Nature*, 325, 341–343, 1987.

Triska, F. J., V. C. Kennedy, and R. J. Avanzino, Retention and transport of nutrients in a third-order stream in northwestern California: Hyporheic process, *Ecology*, 70, 1893–1905, 1989.

Triska, F. J., J. H. Duff, and R. J. Avanzino, Patterns of hydrological exchange and nutrient transformation in hyporheic zone of a gravel-bottom stream: Examining terrestrial-aquatic linkages, *Freshwater Biol.*, *29*, 259–274, 1993a.

Triska, F. J., J. H. Duff, and R. J. Avanzino, The role of water exchange between a stream channel and its hyporheic zone in nitrogen cycling at terrestrial-aquatic interface, *Hydrobiologia*, *251*, 167–184, 1993b.

Valett, H. M., S. G. Fisher, and E. H. Stanley, Physical and chemical characteristics of the hyporheic zone of a Sonoran Desert stream, *J. N. Am. Benthol. Soc.*, *9*, 201–215, 1990.

Valett, H. M., J. A. Morrice, C. N. Dahm, and M. E. Campana, Parent lithology, surface-groundwater exchange, and nitrate retention in headwater streams, *Limnol. Oceanogr.*, *41*, 333–345, 1996.

Vervier, P., M. Dobson, and G. Pinay, Role of interaction zones between surface and ground waters in DOC transport and processing: Considerations for river restoration, *Freshwater Biol.*, *29*, 275–284, 1993.

Wang, H. F., and M. P. Anderson, Introduction to Groundwater Modeling: Finite Difference and Finite Element Methods, W. H. Freeman, New York, 1982.

Wondzell, S. M., and F. J. Swanson, Seasonal and storm dynamics of the hyporheic zone of a 4th-order mountain stream, I, Hydrologic processes, *J. N. Am. Benthol. Soc.*, *15*, 3–19, 1996a.

Wondzell, S. M., and F. J. Swanson, Seasonal and storm dynamics of the hyporheic zone of a 4th-order mountain stream, II, Nitrogen cycling, *J. N. Am. Benthol. Soc.*, *15*, 20–34, 1996b.

Wondzell, S. M., and F. J. Swanson, Floods, channel change, and the hyporheic zone, *Water Resour. Res.*, *35*, 555–567, 1999.

Wroblicky, G. J., M. E. Campana, H. M. Valett, and C. N. Dahm, Seasonal variation in surface-subsurface water exchange and lateral hyporheic area of two stream-aquifer systems, *Water Resour. Res.*, *34*, 317–328, 1998.

———————————

 T. Kasahara, Department of Geography, York University, 4700 Keele Street, Toronto, Ontario, Canada M3J 1P3. (ktamao@yorku.ca)

 S. M. Wondzell, Pacific Northwest Research Station, Olympia Forestry Sciences Laboratory, Olympia, WA 98512, USA. (swondzell@fs.fed.us)